Molecular radiobiology

Regulation of O_2 consumption by the PI3K and mTOR pathways contributes to tumor hypoxia

Catherine J. Kelly [a], Kamila Hussien [a], Emmanouil Fokas [a], Pavitra Kannan [a], Rebecca J. Shipley [b], Thomas M. Ashton [a], Michael Stratford [a], Natalie Pearson [c], Ruth J. Muschel [a,*]

[a] Gray Institute for Radiation Oncology and Biology, Department of Oncology, University of Oxford; [b] Department of Mechanical Engineering, University College London; and [c] Mathematical Institute, University of Oxford, UK

ABSTRACT

Background: Inhibitors of the phosphatidylinositol 3-kinase (PI3K) and the mammalian target of rapamycin (mTOR) pathway are currently in clinical trials. In addition to antiproliferative and proapoptotic effects, these agents also diminish tumor hypoxia. Since hypoxia is a major cause of resistance to radiotherapy, we sought to understand how it is regulated by PI3K/mTOR inhibition.
Methods: Whole cell, mitochondrial, coupled and uncoupled oxygen consumption were measured in cancer cells after inhibition of PI3K (Class I) and mTOR by pharmacological means or by RNAi. Mitochondrial composition was assessed by immunoblotting. Hypoxia was measured in spheroids, in tumor xenografts and predicted with mathematical modeling.
Results: Inhibition of PI3K and mTOR reduced oxygen consumption by cancer cell lines is predominantly due to reduction of mitochondrial respiration coupled to ATP production. Hypoxia in tumor spheroids was reduced, but returned after removal of the drug. Murine tumors had increased oxygenation even in the absence of average perfusion changes or tumor necrosis.
Conclusions: Targeting the PI3K/mTOR pathway substantially reduces mitochondrial oxygen consumption thereby reducing tumor hypoxia. These alterations in tumor hypoxia should be considered in the design of clinical trials using PI3K/mTOR inhibitors, particularly in conjunction with radiotherapy.
© 2014 The Authors. Published by Elsevier Ireland Ltd. Radiotherapy and Oncology 111 (2014) 72–80 This is an open access article under the CC BY-NC-ND license (http://creativecommons.org/licenses/by-nc-nd/3.0/).

Genetic alterations that lead to aberrant activation of the PI3K and mTOR pathways are among the most frequent in cancers of all types [8,40]. PI3K/mTOR pathway signaling promotes a plethora of oncogenic cellular functions including growth and cell survival. As a result, a variety of pharmacologic agents have been developed to inhibit this pathway and are entering clinical trials [25].

In addition to reducing tumor proliferation and survival, we and others have shown that inhibitors of the PI3K pathway greatly diminish tumor hypoxia [14,38,53], a characteristic feature of solid tumors which correlates with poorer prognosis, increased metastasis and resistance to therapeutic intervention, particularly radiotherapy (XRT) [18,33,34]. A variety of strategies to increase tumor oxygenation have been proposed in order to improve the outcome of XRT, including the inhalation of hyperoxic gases [20–23,42], and vascular normalization [10,19,41]. Poor local perfusion is a major contributor to hypoxia, resulting from the disorganized

vasculature, increased interstitial pressures and transient vascular closures commonly found in cancer [50]. Inhibition of PI3K signaling results in improved vascular structure and perfusion [14,38], suggesting that vascular normalization plays a role in the observed reoxygenation. However, potential contributions of alterations in oxygen consumption have not been determined. Mathematical modeling of the roles of supply and demand in tumor oxygenation suggests that reduction of hypoxia is more likely to be accomplished by decreasing tumor oxygen consumption than by improvement of vascular supply [45].

Consistent with this idea, Gallez and colleagues have shown that treatment of some murine tumors with inhibitors of the Epidermal Growth Factor Receptor (EGFR) or with AsO_3 leads to decreased O_2 consumption and hence decreased hypoxia in experimental tumors correlating with enhanced efficacy of XRT [3,12]. The effects of inhibiting PI3K and mTOR on O_2 consumption and tissue oxygenation however, have not been similarly explored.

Here we report that pharmacological and genetic inhibition of PI3K and/or mTOR leads to diminished O_2 consumption in a panel of cell lines from different primary tumors. Using spheroid and

* Corresponding author.
  E-mail address: ruth.muschel@gmail.com (R.J. Muschel).

in vivo models, we found that tissue hypoxia was reduced even in the absence of vascular remodeling by pharmacological inhibition of PI3K/mTOR.

Methods

In vitro studies

The cell lines tested FaDu (human nasopharyngeal), EMT6 (mouse mammary carcinoma), HCT116 (human colorectal) and U87 (human glioma) were chosen because they form spheroids of sufficient size (~400–500 μm diameter) to become hypoxic. Spheroids generated using the liquid overlay technique [9] were treated 6 days after initiation.

Treatments

BEZ235 and BKM120 (Novartis Pharmaceuticals) and AZD8055 (#CT-A8055, ChemieTek) were dissolved in 0.1% DMSO. Control groups were treated with equal amounts of DMSO.

Cell transfections were performed by reverse transfection with Interferin (PolyPlus) using 5 nM short interfering RNA (siRNA) oligonucleotides for PI3K110α (#L-003018), p85β (#L-003021), mTOR (#L-003008) and non-targeting (#D-001810) from Dharmacon RNAi Technologies. Doses in tissue culture were chosen based on the lowest concentration to reduce pAKT repeatably and by at least approximately 3-fold.

Immunoblotting

Antibodies were: pAKT (Ser-573 #9271, 1:1000), pmTOR (Ser-2448 #2971, 1:500), pS6 ribosomal protein (Ser235/236 #4856, 1:1000), all Cell Signalling Technology in 5% Bovine Serum Albumin (BSA); Actin (mAb clone AC-15 #A1978, Sigma, 1:20,000 in 5% milk); OXPHOS complexes (#MS601, Mitosciences, 1:500 in milk); citrate synthase (#CISY-11A, Alpha Diagnostic, 1:500 in milk).

Oxygen consumption

Cells were seeded in 96-well plates from Seahorse Biosciences prior to treatment with inhibitors (24 h) or siRNA (48 h). One hour prior to the assay, culture medium was replaced with modified DMEM (Seahorse Bioscience) supplemented with 5 mM sodium pyruvate, 4 mM glutamine, (pH 7.4). The rate of oxygen consumption (OCR) was measured at 37 °C using an XF96 extracellular analyzer (Seahorse Bioscience). Four measurements were taken before and three after each sequential injection of oligomycin (1 μM), FCCP (0.8 μM) and rotenone and antimycin A (both 1 μM). Plates were fixed with 4% paraformaldehyde (pFA) and stained with Hoechst 33342 (H3570, Invitrogen). Cell number was proportional to fluorescence (Ex 380 nM and Em 450 nM). The OCR linked to coupled respiration was obtained by subtracting OCR after the addition of oligomycin from basal OCR. OCR after addition of the mitochondrial uncoupler FCCP reflected the maximal respiratory rate. Non-mitochondrial respiration was defined as the rate after rotenone/antimycin A application and was subtracted from the basal OCR to determine the mitochondrial OCR. "To account for variations in cell number brought about by drug-induced effects on proliferation or cell death, all raw OCR values were normalized to cell density measurements as determined by Hoechst fluorescence, on a well-by-well basis. At the end of the assay, plates were fixed with 4% paraformaldehyde (pFA), and stained with Hoechst 33342 (2 μg/ml, H3570, Invitrogen) prior to measuring fluorescence (Ex 380 nM and Em 450 nM). The effect of treatment on cell density with BEZ235 or BKM120 varied across cell lines (Supplemental Fig. 1A).

Isolation of mitochondrial-enriched fraction

Mitochondria were isolated as previously described [16,51]. 2×10^7 cells were centrifuged at 750g for 5 min at 4 °C,

resuspended in cold PBS, centrifuged and resuspended in isolation buffer (containing 10 mM Tris–HCl, 0.32 M sucrose, 0.1 mM EGTA, and 1:100 Halt Protease Inhibitor Cocktail. After 10 freeze/thaw cycles (−70 °C for 3 m and 37 °C for 2 min), the homogenates were centrifuged at 700g for 10 min to remove the nuclei and unbroken cells. Supernatants were centrifuged at 12,000g for 10 min to separate the mitochondria and cytosol.

Spheroids

To quantify hypoxia, spheroids were incubated with 200 μM EF5 (2-(2-Nitro-1H-imidazol-1-yl)-N-(2,2,3,3,3-pentafluoropropyl) acetamide), a gift from Cameron Koch's lab) for 6 h at 37 °C, prior to overnight fixation in 4% pFA in PBS and preservation in 30% sucrose in PBS at 4 °C. 8 μm sections were incubated overnight at 4 °C with the EF5 Cy3-conjugated monoclonal antibody ELK3-51 (www.hypoxia-imaging.org) and counterstained with Hoechst 33342. Images were acquired with a Nikon Eclipse 90i with a Hamamatsu ORCA-ER camera. A mask was created for each spheroid using the Hoechst image, prior to measuring the average pixel intensity per spheroid in the background-subtracted EF5 image using ImageJ [1].

To assess signaling inhibition in spheroids, sections were stained with anti-pAKT antibody using ImmPRESS™ reagent kit (MP-7401, VectorLabs) and DAB Peroxidase substrate kit (SK-4100, VectorLabs). Images acquired with a Nikon Eclipse E800 were analyzed for 3,3′-Diaminobenzidine (DAB)-positive pixels semi-automatically using a method described previously [6].

Statistical analysis

Quantitative data were expressed as means ± 95% Confidence Interval. One-way ANOVAs, followed by the Bonferroni post-test, were used to assess the differences among various treatments with Prism 5 (GraphPad Software Inc.), unless otherwise stated.

Mathematical modeling

For simulation of *in vivo* O_2 consumption, 2D vascular networks were generated stochastically [37], using vessel parameter distributions (vessel length, diameter and branching angle) obtained from ex vivo data [14]. The resulting coupled blood flow and O_2 transport problem was solved using code available via Dr. Secomb's website (www.physiology.arizona.edu/people/secomb/greens). A representative base O_2 consumption rate of 1.5 cm³/100 cm³/min was used [46].

In vivo studies

All animal experiments were carried out in accordance with UK Home Office regulations. FaDu cells bearing a HRE-luc reporter (Cignal Lenti HIF Reporter luciferase (SABiosciences)), for hypoxia were described and validated previously [38]. 1×10^6 cells were inoculated subcutaneously in athymic nude mice. Mice were divided into cohorts of $n = 4$ mice per cohort. Drug administration by oral gavage was initiated once tumors reached 100 mm³ volume, as determined using calipers. Tumors were treated for 7 days with BEZ235 at 0, 20 or 30 mg/kg in NMP/PEG300 (Novartis Pharmaceuticals, Basel, Switzerland). Decreases in hypoxia were seen at 3 days with maximal effects by 5–7 days. We failed to observe effects at earlier times. Thus we used 7 days for these experiments. Imaging of hypoxia and perfusion was carried out as previously described [38]. Before sacrifice EF5 was administered as previously described [38]. Tumor tissue was fixed and stained for EF5 and Ki-67. Images were acquired using a Nikon Eclipse E800 microscope with a Nikon DMX1200 digital camera and measured with ImageJ.

Results

PI3K/mTOR inhibition reduced tumor cell oxygen consumption

The O_2 consumption rate (OCR) of cancer cell monolayers (normalized to cell number) was reduced after 24 h treatment with the Class I PI3K inhibitor BKM120 or with the dual PI3K/mTOR inhibitor BEZ235 (Fig. 1A, $P < 0.01$, one-way ANOVA and Supplemental Fig. 1B). A trend for reduced OCR was evident within 5 h of treatment with either inhibitor although this was not uniformly significant (Supplemental Fig. 1C). Functional inhibition of PI3K was demonstrated by dose-dependent reduction in AKT phosphorylation at 24 h (Fig. 1C). Both drugs also reduced the phosphorylation of mTOR and S6. BEZ235 is a direct inhibitor of mTOR.
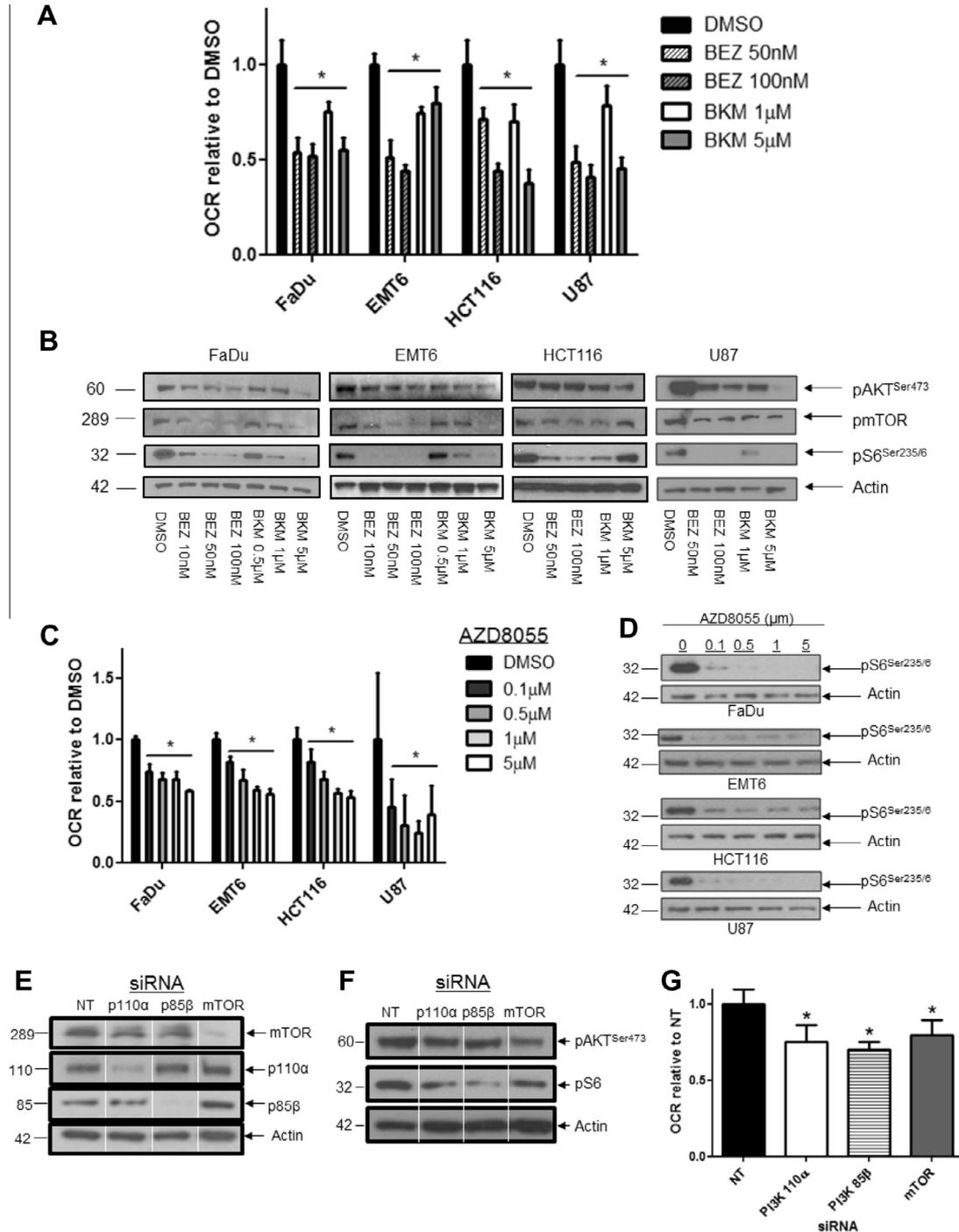
Fig. 1. Inhibition of PI3K and mTOR activities reduces oxygen consumption *in vitro*. (A) Effect of dual PI3K/mTOR inhibitor BEZ235 and single Class I PI3K inhibitor BKM120 on cellular oxygen consumption rate (OCR). FaDu, EMT6, HCT116 and U87 cells were treated as indicated for 24 h. Total cellular oxygen consumption rate (OCR) was calculated in $n = 12$ wells. Data shown are representative of three independent experiments. (B) Immunoblotting confirmed reduction in signaling through the PI3K/mTOR pathway in monolayers treated with BEZ235 or BKM120 for 4 h (12 h and 24 h for HCT116 and U87 respectively). (C) Treatment for 24 h with the mTOR inhibitor AZD8055 decreased OCR. (D) Immunoblotting for pS6 confirmed AZD8055 reduced mTOR signaling. (E) Immunoblots for mTOR, the PI3K subunits p110α and p85β, and Actin in FaDu cells transfected with non-targeting (NT) and PI3K, mTOR siRNA for 3 days, demonstrate that target protein levels were reduced. (F) Immunoblots for pAKT and pmTOR in transfected cells show reduced signaling through the PI3K/mTOR pathway. (G) FaDu cells transfected with PI3K p110α, p85β or mTOR siRNA exhibit reduced mitochondrial OCR compared with those transfected with NT siRNA. All data points represent mean ± 95% Confidence Interval. One-way ANOVAs were performed with Bonferroni-corrected post *t*-tests comparing treated to DMSO-treated control samples. *$P < 0.01$. Data shown are representative of three independent experiments.

However since mTOR is also a downstream target of PI3K, the decrease in pmTOR and pS6 seen with BKM120, a specific PI3K inhibitor is not unexpected. Thus the use of the specific PI3K inhibitor BKM120 does not preclude mTOR as a target. mTOR can also feedback onto PI3K and AKT pathways. The OCR in cells treated with the direct mTOR inhibitor AZD8055 was also reduced in a dose-dependent fashion (Fig. 1C and D). Treatment with rotenone and antimycin A, which block mitochondrial electron transport, inhibited the O_2 consumption by these cells (FaDu 82.9%; EMT6 91.1%; HCT116 79%; U87 75%) showing that mitochondrial respiration accounted for the preponderance of O_2 consumption. Thus treatment with PI3K/mTOR inhibitors diminished the mitochondrial O_2 consumption in a variety of cancer cells.

In addition, we reduced signaling in FaDu cells by genetic means (Fig. 1E and F). RNAi against PI3K 85β (regulatory domain) and PI3K 110α (catalytic domain) reduced their respective protein levels and depressed signaling as measured by pAKT and pS6 levels. RNAi against mTOR reduced its protein levels and also depressed the signaling through S6. O_2 consumption in PI3K and mTOR-silenced cells was reduced by 25–30% compared to the non-targeted control (Fig. 1G). Thus genetic interference with the PI3K signaling pathway also reduced O_2 consumption as did pharmacological inhibition.

The PI3K/mTOR pathway is a promoter of glycolytic metabolism [13,52]. In the cell lines tested, treatment with BKM120 reduced glycolysis. However, BEZ235 inhibited glycolysis in some cell lines, but not in others (Supplementary Fig. 1D). Because mitochondrial oxygen consumption can be limited by substrate availability through glycolysis, glucose-free medium supplemented with pyruvate and glutamine was used for the above OCR measurements.

PI3K/mTOR inhibition reduce mitochondrial function, not protein

We examined the possibility that a reduction in mitochondrial mass might contribute to decreased O_2 consumption. However, the levels of citrate synthase, a component of the Krebs cycle frequently used to monitor mitochondrial mass, remained unchanged after treatment with either inhibitor (Fig. 2A and Supplementary Fig. 2A). Levels of electron transport chain (ETC) complexes I, IV and V (ATP synthase) increased in the mitochondrial fraction of FaDu cells treated with BEZ235 or BKM120 compared to the control (Fig. 2B), confirming that the mitochondrial amounts were not reduced.

We next looked at the effect of BEZ235 and BKM120 on mitochondrial bioenergetics. In a normally functioning cell, the rate of cellular O_2 consumption (as shown in Fig. 1A) is determined by the activity of the electron transport chain (ETC) and the rate of ATP production, with these processes 'coupled' via the proton gradient (Fig. 2C). In addition to this, proton leakage and non-mitochondrial also contribute. To assess the specific contributions of ATP synthesis and ETC activity to altered O_2 consumption, we compared respiration in both the coupled and uncoupled states through sequential addition of oligomycin (an ATP synthase inhibitor) and FCCP (which dissipates the proton gradient) (Fig. 2D). Coupled respiration was reduced by BEZ235 or BKM120 treatment in all cell lines (Fig. 2E). However, as coupled respiration is dependent on the supply of electrons from the ETC, this does not in itself show that the reduction is dependent on ATP synthase activity. Hence it is necessary to also consider uncoupled respiration, which reflects ETC activity. Treatment with BEZ235 or BKM120 reduced uncoupled respiration in the human cells lines (FaDu, HCT116 and U87), although the effect was smaller than that observed for coupled respiration (Fig. 2F). Thus both coupled and uncoupled respiration are inhibited by PI3K/mTOR inhibition.

Decreased oxygen consumption corresponds to a substantial improvement in 3D oxygenation

To evaluate whether the results in monolayers could translate to a 3D tissue environment, we examined hypoxia within spheroids. Inhibition of PI3K in FaDu and EMT6 spheroids was demonstrated by reduction of pAKT staining after drug treatment (Fig. 3A and B). Spheroids of 450–500 μm diameter were treated for 24 or 48 h with either DMSO, BEZ235 (50 nM) or BKM120 (5 μM). Hypoxia that was evident in the control spheroids, as indicated by EF5 staining, was reduced in spheroids treated with either BEZ235 or BKM120 (Fig. 3C and D). These spheroids were smaller than the controls (Supplementary Fig. 3A), suggesting proliferation was affected by the inhibitors. As EF5 binds only in viable cells, there was the possibility that cell death accounted for the reduction in signal. To examine this possibility, the spheroids were returned to drug-free medium after 24 h of drug treatment. Hypoxia recurred, demonstrating viability with the exception of BKM120-treated FaDu spheroids. (Fig. 3C and E) ($p < 0.01$, two-way ANOVA). Dose-dependent reductions in hypoxia were also observed in HCT116 spheroids (Supplementary Fig. 3B). Thus decreased O_2 consumption due to PI3K/mTOR inhibition leads to decreased hypoxia in spheroids.

Reduction in hypoxia in treated tumors is consistent with impaired oxygen consumption

The findings using spheroids presented above support the hypothesis that reduction of oxygen consumption due to PI3K/mTOR inhibition would result in a reduction of tumor hypoxia in vivo. Additionally since spheroids are avascular, their use bypasses the complexities of the tumor vasculature. To evaluate the effect that reduced O_2 consumption might have in the context of abnormal vasculature, we used a mathematical modeling approach developed by Secomb et al. [46]. 2D and 3D vascular networks were generated in silico, derived from serial confocal images of xenografts from the FaDu cell line [14]. Simulations of blood flow through these vascular networks were combined with factors for the rate of O_2 diffusion and O_2 consumption by the surrounding tissue. Fig. 3F and G show oxygen distributions in one such vascular network using two different rates of O_2 consumption (maximum and 55% of maximum, the latter observed in FaDu cells treated with 100 nM BEZ235). Using this model we calculated the mean hypoxic fraction from 10 different vascular networks observed in FaDu tumors across a range of decrements in O_2 consumption rates (Fig. 3H). A decrease of 20% in oxygen consumption would be predicted to decrease the mean hypoxic fraction by one-third, based on this model. Thus smaller reductions of O_2 consumption than the maximal observed in the monolayer would be predicted to be medically significant.

To test our predictions, we treated mice bearing FaDu HRE-Luc xenografts with BEZ235 at two different doses (20 mg/kg and 30 mg/kg). Both doses significantly reduced the luciferase signal compared to the untreated tumors (Fig. 4A). Reduction in hypoxia was confirmed through EF5 staining (Fig. 4B). We have previously demonstrated that administration of 20 mg/kg BEZ235 results in a greater density of normalized blood vessels and increased perfusion in FaDu xenograft [14]. However PI3K inhibition with BEZ235 or other drugs at higher doses has been reported to lead to blood vessel destruction in tumors [14,17,24]. Tumors treated with 30 mg/kg BEZ235 had no increase in perfusion compared to the control (Fig. 4C), but still demonstrated a substantial reduction in hypoxia. Both doses led to greater than 5-fold reduction of pAKT or pS6 staining (Fig. 4D). However the lower dose did not reduce proliferation of the tumor cells while the higher dose had a strong
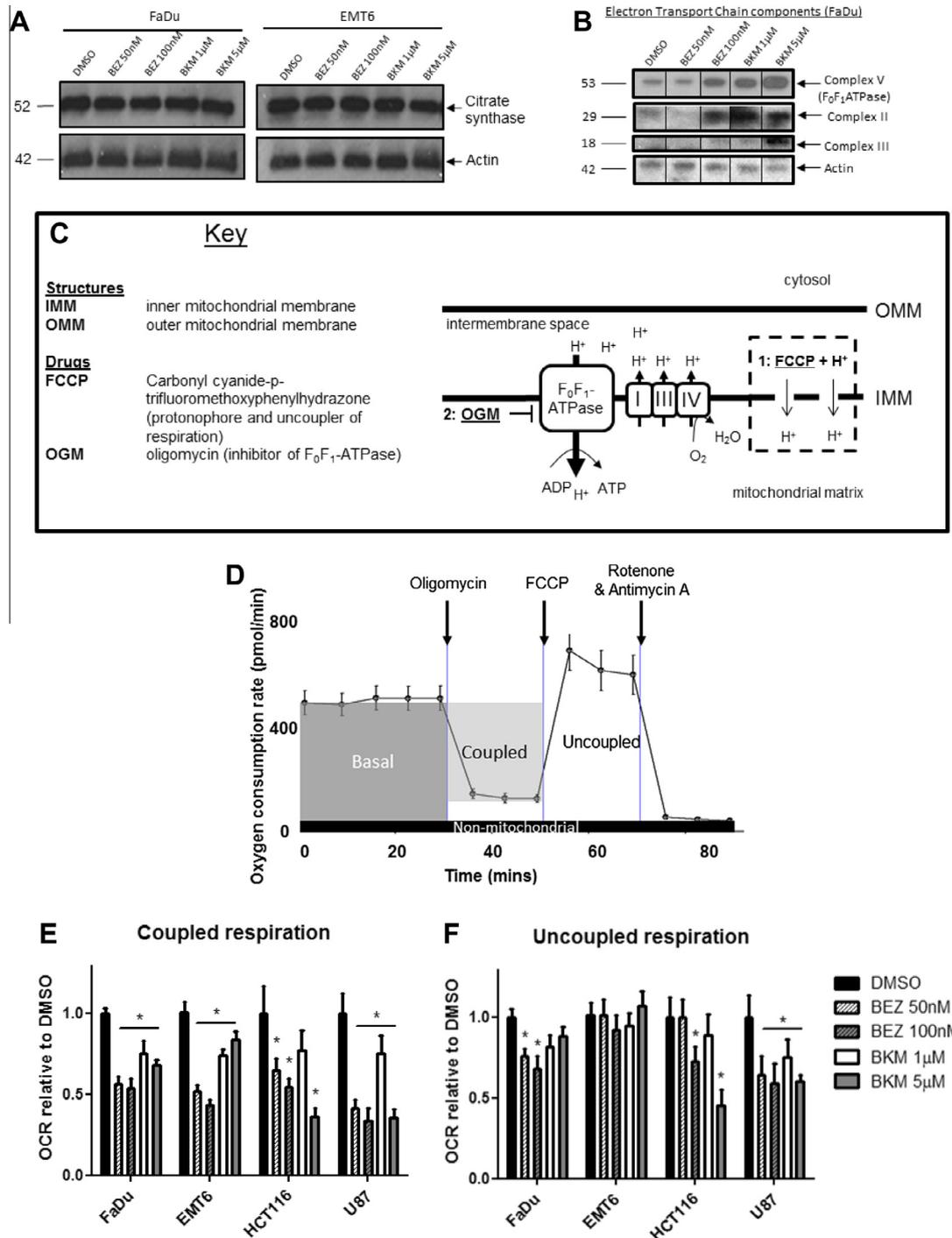
Fig. 2. Decrease in oxygen consumption correlates with a decline in mitochondrial function. (A) Mitochondrial mass in FaDu and EMT6 cells treated for 24 h with BEZ235 and BKM120 was unaffected, as confirmed by immunoblotting for citrate synthase. (B) Levels of the electron transport chain (ETC) complexes II, III and V (F_0F_1-ATPase) increased in FaDu mitochondria treated with BEZ235 and BKM120 compared to the DMSO-treated control (Ctl). (C) The functionality of mitochondria is dependent on the constant cycling of protons (H+) between the intermembrane space and the mitochondrial matrix. The inner and outer mitochondrial membranes (IMM and OMM) act as barriers to H+ transport. Movement of protons into the intermembrane space by the ETC complexes results in a mitochondrial membrane potential (MMP) which is relieved by F_0F_1-ATPase during the generation of ATP. Alterations to the MMP indicate a change in this flux. Mitochondrial function can be disrupted by the addition of (1) FCCP, which dissipates the H+ gradient and the MMP, uncoupling respiration from ATP production and enabling it to occur at its maximal rate; (2) Oligomycin, which inhibits F_0F_1-ATPase, enables calculation of ATP-dependent (coupled) respiration. (D) Coupled and uncoupled respiration were determined in cells to which either FCCP or oligomycin (respectively) had been added. Subtraction of the post-oligomycin OCR from the basal OCR gives coupled respiration. Uncoupled respiration is determined by subtracting the post-rotenone (non-mitochondrial) OCR from the post-FCCP OCR. (E and F) Coupled respiration was significantly reduced in all cell lines after 24 h treatment with BEZ235 or BKM120 compared to the DMSO-treated control. The effect of treatment with BEZ235 or BKM120 on uncoupled respiration varied across cell lines. All data points represent mean ± 95% Confidence Interval in $n = 12$ wells. Data shown are representative of three independent experiments. One-way ANOVAs were performed with Bonferroni-corrected post t-tests comparing treated to DMSO-treated control samples. $^*P < 0.01$.

antiproliferative effect on the tumor cells without noticeable histological evidence of necrosis (Fig. 4D, quantified in Fig. 4E). Reduced proliferation at the higher, but not the lower, dose was reflected in growth curves (Supplemental Fig. 4). Both doses resulted in decreased hypoxia. Treatment of mice with tumors with BEZ235 at the higher dose led to decreased hypoxia despite no change in
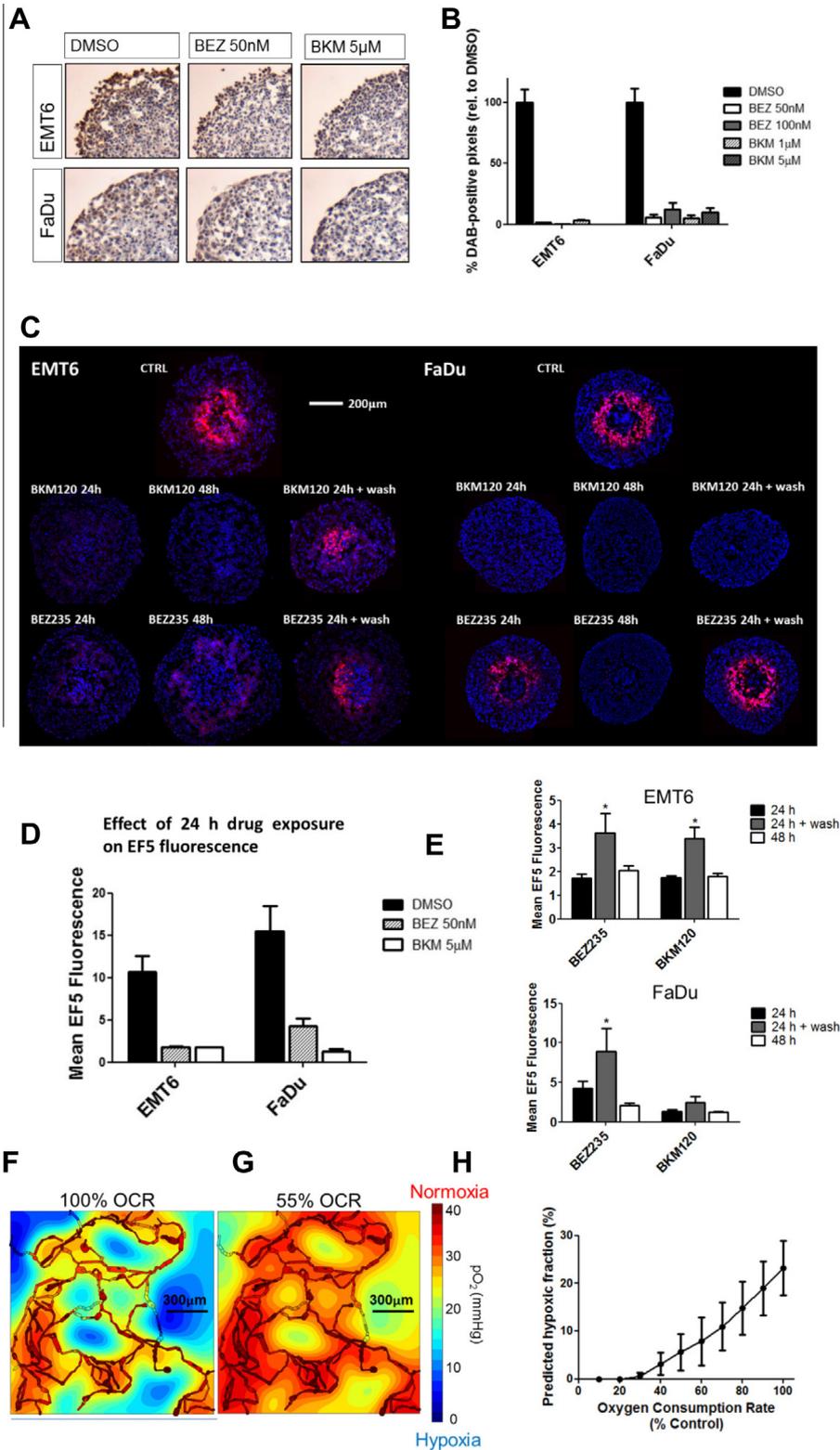
Fig. 3. Hypoxia is reduced in a 3D spheroid model and is predicted to decline *in vivo*. (A) EMT6 and FaDu spheroids were treated for 24 h with BEZ235 or BKM120, prior to fixation and sectioning. Sections were DAB-stained for pAKT (Ser473) expression. Representative images are shown for BEZ235 (50 nM) and BKM120 (5 μM). (B) The percentage of DAB-positive pixels in the viable region of the spheroid was reduced with all treatments. (C) Spheroids were treated with 50 nM BEZ235 or 5 μM BKM120 for 24 h, 48 h or 24 h followed by 24 h incubation in drug-free medium (24 h + wash). Hypoxia was assessed by staining central spheroid sections for EF5 (red) with Hoechst as a counterstain (blue). Data shown are representative of two independent experiments, n = 10 spheroids. (D) Mean EF5 fluorescence in spheroids treated for 24 h was reduced in both cell lines tested. (E) To assess whether hypoxia was recoverable, mean EF5 fluorescence in spheroids treated for 24 h was compared with that in spheroids treated for either 48 h or 24 h followed by the 24 h wash in drug-free medium. In cells treated with BEZ235, the 24 h wash period led to a return of the hypoxia signal. (F and G) Simulated distribution of oxygen partial pressure (mmHg) in a representative 1497 μm × 1482 μm vascular network derived from *ex vivo* samples where oxygen consumption was either 100% (F) or 55% (G) of base level. Highly oxygenated regions are in red, scaling down to poorly oxygenated regions in blue. (H) Average hypoxic fraction (defined as <10 mmHg) calculated across 10 example networks as in F as a function of varying oxygen consumption. All data points represent mean ± 95% Confidence Interval. One-way ANOVAs were performed with Bonferroni-corrected post t-tests. *P < 0.01.
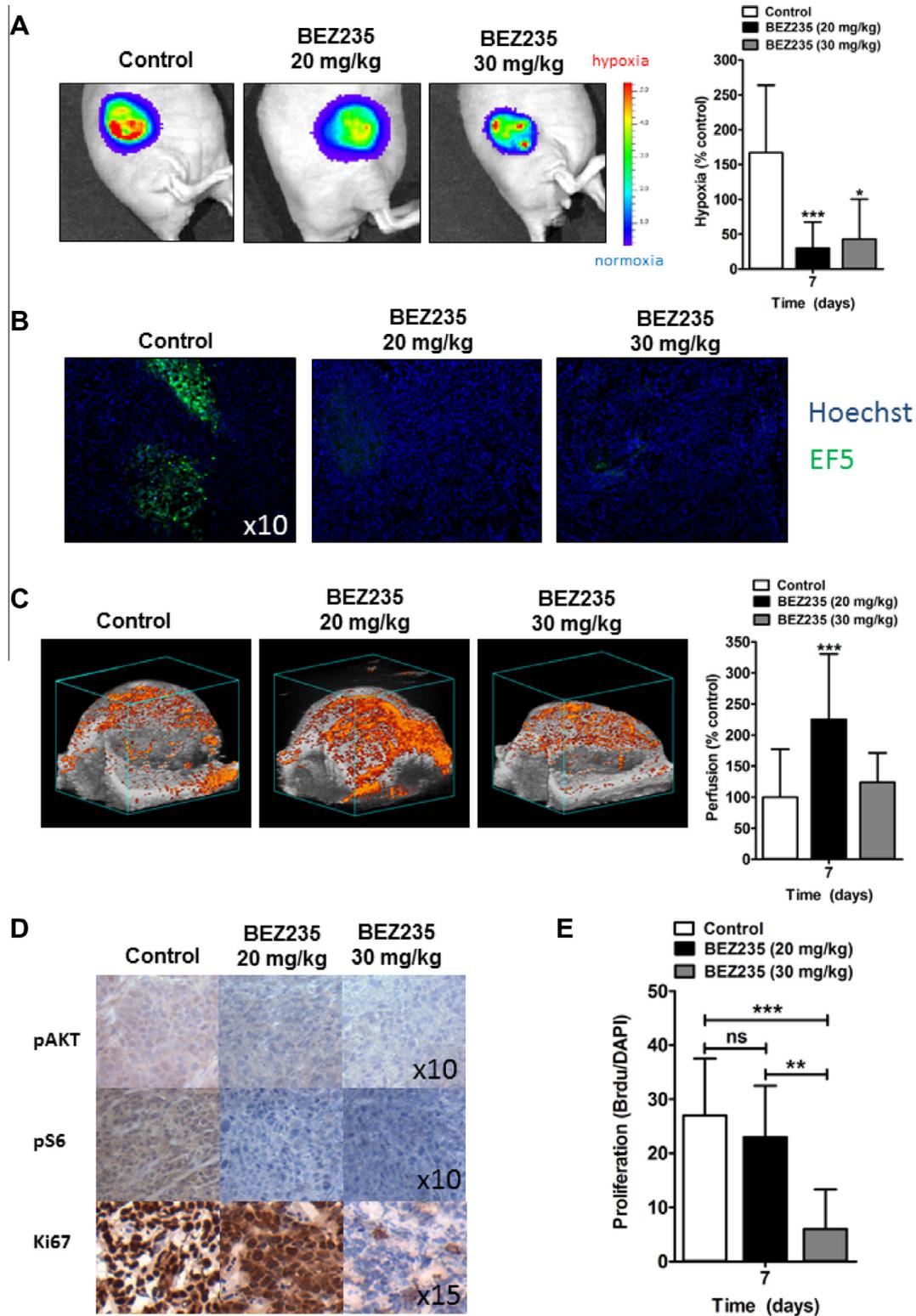
Fig. 4. BEZ235 reduces hypoxia *in vivo* in the absence of vascular normalization. Xenograft tumors from the FaDu cell line with a stably expressed hypoxia-dependent luciferase signal were grown in athymic nude mice. Mice were divided into cohorts of $n = 4$ mice per cohort. Tumors were treated for 7 days with BEZ235 at 0, 20 or 30 mg/kg. (A) Hypoxia was monitored by bioluminescent imaging of the luciferase signal. Representative images and hypoxia measurements from FaDu tumors at day 7 treated with BEZ235 at doses indicated show that the hypoxia signal is reduced with BEZ235 treatment. (B) Immunostaining for EF5 (green) in FaDu tumors independently confirmed the reduction in hypoxia (10× magnification). (C) Perfusion as depicted by microbubbles (orange signal), was evaluated in the entire tumor at day 7 after treatment with BEZ235 as indicated. Increased perfusion, indicative of vascular normalization, was present in tumors treated with 20 mg/kg, but not 30 mg/kg, BEZ235. Columns, mean; bars, 95% CI. (D) Evaluation of the effects of BEZ235 on pAKT, pS6 and the proliferation marker Ki-67 in FaDu tumors. Sections were stained with the indicated antibodies. Both doses of BEZ235 reduced signaling through the PI3K/mTOR pathway, but only the higher dose (30 mg/kg) of BEZ235 reduced proliferation. Magnification as shown in image (E). Columns, mean; bars, 95% CI, *$P < 0.05$, **$P < 0.01$, ***$P < 0.001$, over vehicle-treated control.

overall perfusion consistent with the hypothesis that BEZ235 induced decreased hypoxia due to reduced O_2 consumption independent of alterations in perfusion.

Altogether, our findings indicate that alterations to cellular O_2 consumption could have a significant impact on tumor hypoxia, in agreement with previous *in vivo* observations [3,12].

Discussion

In this study we show that pharmacological or genetic inhibition of the PI3K/mTOR pathway reduces mitochondrial O_2 consumption in a panel of cancer cell lines. As a consequence, pharmacological inhibition of PI3K reduces hypoxia in spheroids and tumor xenografts.

Several groups including our own have found that PI3K inhibition can lead to vascular normalization, correlating with decreased hypoxia [14,38,43]. However, our findings here suggest that reducing cellular O_2 consumption through PI3K inhibition can additionally have a significant effect on hypoxia. It is likely that *in vivo* changes in hypoxia mediated by PI3K inhibition result from a synergy of the increased blood flow and reduced respiration.

In agreement with our findings, reduced O_2 consumption after direct inhibition of the PI3K/mTOR pathway [26,32,35], or after the withdrawal or inhibition of growth factors which act via the pathway has been previously reported [3,32,49]. However there is no consensus on how the pathway regulates oxidative respiration. PI3K/AKT/mTOR signaling can be hypothesized to enhance respiration through multiple mechanisms, including substrate generation, metabolite transport across the mitochondrial membrane and activity of the mitochondrial machinery. While increased mitochondria biogenesis is one means of generating increased oxidative metabolism, we failed to detect evidence of a decrease in overall mitochondria mass in treated cells with unchanged levels of citrate synthase and increased levels of mitochondrial complexes. However we did not examine mitochondrial numbers, morphology or location. In our measurements of oxygen consumption, excess pyruvate and glutamine were used to saturate the reaction, removing substrate limitations. However, substrate availability could still play a role in spheroids or *in vivo*, particularly through glycolysis. Amounts of the glucose transporter GLUT1 may be reduced after PI3K/AKT/mTOR inhibition [7,11,36,39,48]. Localization of hexokinase II to the mitochondria where it couples glycolysis to ATP synthesis, enhancing glycolytic flux, is also reduced by mTOR and AKT inhibition [2,4,31].

Accessibility of ADP and ATP to the mitochondrial matrix could be a point of regulation of mitochondrial oxygen consumption as well. ADP and ATP enter the mitochondria through the outer mitochondrial membrane via the voltage dependent anion channel (VDAC). ADP/ATP flow to and from mitochondrial ATP synthase is essential to relieve the proton gradient set up by the ETC, enabling electron transport and O_2 consumption. Consistent with involvement of ADP/ATP transport or turnover, mitochondrial hyperpolarization, caused by a buildup of this gradient, has been reported in both AKT- and mTOR complex 2-deficient cells and after treatment with the mTOR inhibitor rapamycin [4,35]. It is possible that the PI3K/mTOR pathway regulates VDAC. Localization of mTOR and its target Ser473-phosphorylated AKT to VDAC1 are increased after growth factor stimulation [4] and conductance through the channel is negatively regulated by the AKT target glycogen synthase kinase 3β (GSK3β) [28,47,5].

Finally, F_0F_1-ATP synthase may be regulated by PI3K/AKT/mTOR signaling. Active AKT interacts with ATP synthase [5,54] and its subunits contain consensus sequences for AKT binding [26]. In $PTEN^{-/-}$ cells, activated AKT binds the α and β subunits of ATP synthase to stimulate activity [26]. Activated AKT may therefore directly control the rate of ATP synthesis, and therefore oxygen consumption, through phosphorylation of ATP synthase. "Further work will be needed to elucidate the biochemical mechanisms that lead to alterations in oxygen metabolism and to determine potential relationships to proliferation. Of course cell death itself could decrease oxygen consumption. We attempted to control for toxicity through normalization for cell death in tissue culture, by noting that the effect is reversible in spheroids and that *in vivo* at the lower dose the extent of proliferation in similar to controls."

Decreased hypoxia in tumors treated with PI3K/mTOR inhibition would be expected to lead to increased sensitivity to radiation. This expectation is confirmed since pharmacological inhibition of PI3K, mTOR and dual PI3K/mTOR inhibition have all been reported to increase sensitivity to DNA damaging agents in murine cancer models [15,27,30,44]. We showed enhanced tumor growth delay in response to radiation after treatment with BEZ325 correlating with decreased hypoxia. However it is more difficult to determine to what extent alleviation of hypoxia accounts for these results, because these inhibitors also sensitize cells to DNA damage under oxic conditions. Inhibition of PI3K reduces DNA damage repair, but BEZ235 also has off-target effects of inhibition of ATR and DNA-PK [29]. Fokas et al. attempted to separate the effects on tumor oxygenation from cell-specific effects by administering the drug BEZ235 immediately before tumor radiation, when it still altered tumor signaling but before the more prolonged changes of hypoxia associated with extended preincubation had occurred. This study however showed a substantial sensitization resulting from the addition of BEZ235 to radiation. Approximately 1/3 of the effect of sensitization resulted, suggesting that both alterations in hypoxia and direct effects on tumor cell sensitization are at work [14]. Nonetheless both mechanisms could contribute to radiosensitization which could be of clinical significance.

In this study, we have demonstrated for the first time that inhibition of the PI3K/mTOR pathway reduces cellular oxygen consumption and leads to reoxygenation of tumor tissue independent of vascular effects. In light of our findings, ongoing clinical trials with PI3K/mTOR pathway inhibitors are likely to be having substantial effects on tumor hypoxia. Because hypoxia greatly reduces the efficacy of radiotherapy a combination of radiation therapy with PI3K/mTOR inhibition may be beneficial.

Appendix A. Supplementary data

Supplementary data associated with this article can be found, in the online version, at http://dx.doi.org/10.1016/j.radonc.2014.02.007.

References

[1] Abramoff MD, Magelhaes PJ, Ram SJ. Image processing with ImageJ. Biophoton Int 2004;11:36–42.
[2] Ahn KJ, Hwang HS, Park JH, et al. Evaluation of the role of hexokinase type II in cellular proliferation and apoptosis using human hepatocellular carcinoma cell lines. J Nucl Med 2009;50:1525–32.
[3] Ansiaux R, Dewever J, Grégoire V, Feron O, Jordan BF, Gallez B. Decrease in tumor cell oxygen consumption after treatment with vandetanib (ZACTIMA; ZD6474) and its effect on response to radiotherapy. Radiat Res 2009;172:584–91.
[4] Betz C, Stracka D, Prescianotto-Baschong C, Frieden M, Demaurex N, Hall MN. MTOR complex 2-AKT signaling at mitochondria-associated endoplasmic reticulum membranes (MAM) regulates mitochondrial physiology. Proc Natl Acad Sci U S A 2013;110:12526–34.
[5] Bijur GN, Jope RS. Rapid accumulation of AKT in mitochondria following phosphatidylinositol 3-kinase activation. J Neurochem 2003;87:1427–35.
[6] Brey EM, Lalani Z, Johnston C, et al. Automated selection of DAB-labeled tissue for immunohistochemical quantification. J Histochem Cytochem 2003;51:575–84.
[7] Buller CL, Loberg RD, Fan MH, et al. A GSK-3/TSC2/mTOR pathway regulates glucose uptake and GLUT1 glucose transporter expression. Am J Physiol Cell Physiol 2008;295:C836–43.

[8] Cantley LC. The phosphoinositide 3-kinase pathway. Science 2002;296:1655–7.

[9] Carlsson J, Yuhas JM. Liquid-overlay culture of cellular spheroids. Recent Results Cancer Res 1984;95:1–23.

[10] Cerniglia GJ, Pore N, Tsai JH, et al. Epidermal growth factor receptor inhibition modulates the microenvironment by vascular normalization to improve chemotherapy and radiotherapy efficacy. PLoS One 2009;4:e6539.

[11] Chen C, Pore N, Behrooz A, Ismail-Beigi F, Maity A. Regulation of glut1 mRNA by hypoxia-inducible factor-1. Interaction between H-ras and hypoxia. J Biol Chem 2001;276:9519–25.

[12] Diepart C, Karroum O, Magat J, et al. Arsenic trioxide treatment decreases the oxygen consumption rate of tumor cells and radiosensitizes solid tumors. Cancer Res 2011;72:482–90.

[13] Elstrom RL, Bauer DE, Buzzai M, et al. AKT stimulates aerobic glycolysis in cancer cells. Cancer Res 2004;64:3892–9.

[14] Fokas E, Im JH, Hill S, et al. Dual inhibition of the PI3K/mTOR pathway increases tumor radiosensitivity by normalizing tumor vasculature. Cancer Res 2012;72:239–48.

[15] Fokas E, Yoshimura M, Prevo R, et al. NVP-BEZ235 and NVP-BGT226, dual phosphatidylinositol 3-kinase/mammalian target of rapamycin inhibitors, enhance tumor and endothelial cell radiosensitivity. Radiat Oncol 2012;7:48.

[16] Garcia-Cao I, Song MS, Hobbs RM, et al. Systemic elevation of PTEN induces a tumor-suppressive metabolic state. Cell 2012;149:49–62.

[17] Garlich JR, De P, Dey N, et al. A vascular targeted pan phosphoinositide 3-kinase inhibitor prodrug, SF1126, with antitumor and antiangiogenic activity. Cancer Res 2008;68:206–15.

[18] Gray LH, Conger AD, Ebert M, Hornsey S, Scott OC. The concentration of oxygen dissolved in tissues at the time of irradiation as a factor in radiotherapy. Br J Radiol 1953;26:1638–48.

[19] Jain RK. Normalization of tumor vasculature: an emerging concept in antiangiogenic therapy. Science 2005;307:5.

[20] Janssens GO, Rademakers SE, Terhaard CH, et al. Accelerated radiotherapy with carbogen and nicotinamide for laryngeal cancer: results of a phase III randomized trial. J Clin Oncol 2012;30:1777–83.

[21] Kaanders JH, van der Bussink J, Kogel AJ. ARCON: a novel biology-based approach in radiotherapy. Lancet Oncol 2002;12:728–37.

[22] Kaanders JH, Pop LA, Marres HA, et al. Accelerated radiotherapy with carbogen and nicotinamide (ARCON) for laryngeal cancer. Radiother Oncol 1998;48:115–22.

[23] Kaanders JHAM, Bussinka J, van der Kogel AJ. Clinical studies of hypoxia modification in radiotherapy. Semin Radiat Oncol 2004;14:233–40.

[24] Kong D, Okamura M, Yoshimi H, Yamori T. Antiangiogenic effect of ZSTK474, a novel phosphatidylinositol 3-kinase inhibitor. Eur J Cancer 2009;45:857–65.

[25] Kurtz JE, Ray-Coquard I. PI3 kinase inhibitors in the clinic: an update. Anticancer Res 2012;32:2463–70.

[26] Li C, Li Y, He L, et al. PI3K/AKT signaling regulates bioenergetics in immortalized hepatocytes. Free Radic Biol Med 2013;60:29–40.

[27] Manegold PC, Paringer C, Kulka U, et al. Antiangiogenic therapy with mammalian target of rapamycin inhibitor RAD001 (Everolimus) increases radiosensitivity in solid cancer. Clin Cancer Res 2008;14:892–900.

[28] Martel C, Allouche M, Esposti DD, et al. Glycogen synthase kinase 3-mediated voltage-dependent anion channel phosphorylation controls outer mitochondrial membrane permeability during lipid accumulation. Hepatology 2013;57:93–102.

[29] Mukherjee B, Tomimatsu N, Amancherla K, Camacho CV, Pichamoorthy N, Burma S. The dual PI3K/mTOR inhibitor NVP-BEZ235 is a potent inhibitor of ATM- and DNA-PKcs-mediated DNA damage responses. Neoplasia 2012;14:34–43.

[30] Nassim R, Mansure JJ, Chevalier S, Cury F, Kassouf W. Combining mTOR inhibition with radiation improves antitumor activity in bladder cancer cells in vitro and in vivo: a novel strategy for treatment. PLoS One 2013;8:e65257.

[31] Neary CL, Pastorino JG. AKT inhibition promotes hexokinase 2 redistribution and glucose uptake in cancer cells. J Cell Physiol 2013;228:1943–8.

[32] Nogueira V, Park YC, Chen CC, Xu PZ, Chen ML, Tonic I, et al. AKT determines replicative senescence and oxidative or oncogenic premature senescence and sensitizes cells to oxidative apoptosis. Cancer Cell 2008;14:458–70.

[33] Nordsmark M, Overgaard M, Overgaard J. Pretreatment oxygenation predicts radiation response in advanced squamous cell carcinoma of the head and neck. Radiother Oncol 1996;41:31–9.

[34] Overgaard J. Hypoxic radiosensitization: adored and ignored. J Clin Oncol 2007;25:4066–74.

[35] Paglin S, Lee NY, Nakar C, et al. Rapamycin-sensitive pathway regulates mitochondrial membrane potential, autophagy, and survival in irradiated MCF-7 cells. Cancer Res 2005;2005:11061–70.

[36] Pore N, Jiang Z, Shu H-K, Bernhard EJ, Kao GD, Maity A. AKT1 activation can augment hypoxia-inducible factor-1α expression by increasing protein translation through a mammalian target of rapamycin-independent pathway. Mol Cancer Res 2006;4:471–9.

[37] Pries AR, Secomb TW, Gaehtgens P, Gross JF. Blood flow in microvascular networks. Experiments and simulation. Circ Res 1990;67:826–34.

[38] Qayum N, Muschel RJ, Im JH, et al. Tumor vascular changes mediated by inhibition of oncogenic signaling. Cancer Res 2009;69:6347–54.

[39] Radhakrishnan P, Baraneedharan U, Veluchamy S, et al. Inhibition of rapamycin-induced AKT activation elicits differential antitumor response in head and neck cancers. Cancer Res 2013;73:1118–27.

[40] Samuels Y, Wang Z, Bardelli A, et al. High frequency of mutations of the PIK3CA gene in human cancers. Science 2004;304:554.

[41] Sato Y. Persistent vascular normalization as an alternative goal of anti-angiogenic cancer therapy. Cancer Sci 2011;102:1253.

[42] Saunders M, Dische S. Clinical results of hypoxic cell radiosensitisation from hyperbaric oxygen to accelerated radiotherapy, carbogen and nicotinamide. Br J Cancer 1996;27:5271–8.

[43] Schnell CR, Stauffer F, Allegrini PR, et al. Effects of the dual phosphatidylinositol 3-kinase/mammalian target of rapamycin inhibitor NVP-BEZ235 on the tumor vasculature: implications for clinical imaging. Cancer Res 2008;68:6598–607.

[44] Konstantinidou G, Bey EA, Rabellino A, Schuster K, Maira MS, Gazdar AF, et al. Dual phosphoinositide 3-kinase/mammalian target of rapamycin blockade is an effective radiosensitizing strategy for the treatment of non-small cell lung cancer harboring K-RAS mutations. Cancer Res 2009;69:7644–52.

[45] Secomb TW, Hsu R, Ong ET, Gross JF, Dewhirst MW. Analysis of the effects of oxygen supply and demand on hypoxic fraction in tumors. Acta Oncol 1995;34:313–6.

[46] Secomb TW, Hsu R, Park EY, Dewhirst MW. Green's function methods for analysis of oxygen delivery to tissue by microvascular networks. Ann Biomed Eng 2004;32:1519–29.

[47] Sheldon KL, Maldonado EN, Lemasters JJ, Rostovtseva TK, Bezrukov SM. Phosphorylation of voltage-dependent anion channel by serine/threonine kinases governs its interaction with tubulin. PLoS One 2011;6:e25539.

[48] Taha C, Liu Z, Jin J, Al-Hasani H, Sonenberg N, Klip A. Opposite translational control of GLUT1 and GLUT4 glucose transporter mRNAs in response to insulin. Role of mammalian target of rapamycin, protein kinase b, and phosphatidylinositol 3-kinase in GLUT1 mRNA translation. J Biol Chem 1999;274:33085–91.

[49] Vander Heiden MG, Chandel NS, Li XX, Schumacker PT, Colombini M, Thompson CB. Outer mitochondrial membrane permeability can regulate coupled respiration and cell survival. Proc Natl Acad Sci U S A 2000;97:4666–71.

[50] Vaupel P. Tumor microenvironmental physiology and its implications for radiation oncology. Semin Radiat Oncol 2004;14:198–206.

[51] Wieckowski MR, Giorgi C, Lebiedzinska M, Duszynski J, Pinton P. Isolation of mitochondria-associated membranes and mitochondria from animal tissues and cells. Nat Protoc 2009;4:1582–90.

[52] Wieman HL, Wofford JA, Rathmell JC. Cytokine stimulation promotes glucose uptake via phosphatidylinositol-3 kinase/AKT regulation of Glut1 activity and trafficking. Mol Biol Cell 2007;18:1437–46.

[53] Xue Q, Hopkins B, Perruzzi C, Udayakumar D, Sherris D, Benjamin LE. Palomid 529, a novel small-molecule drug, is a TORC1/TORC2 inhibitor that reduces tumor growth, tumor angiogenesis, and vascular permeability. Cancer Res 2008;68:9551–7.

[54] Yang JY, Yeh HY, Lin K, Wang PH. Insulin stimulates AKT translocation to mitochondria: implications on dysregulation of mitochondrial oxidative phosphorylation in diabetic myocardium. J Mol Cell Cardiol 2009;46:919–26.